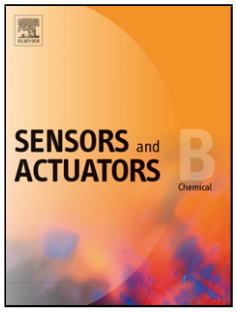

Title: A microfluidic flow-through chip integrated with reduced graphene oxide transistor for influenza virus gene detection

Authors: Chunyu Chan, Jinyu Shi, Yadi Fan, Mo Yang

PII: S0925-4005(17)30970-X
DOI: http://dx.doi.org/doi:10.1016/j.snb.2017.05.147
Reference: SNB 22431

To appear in: *Sensors and Actuators B*

Received date: 13-1-2017
Revised date: 3-5-2017
Accepted date: 24-5-2017

Please cite this article as: Chunyu Chan, Jinyu Shi, Yadi Fan, Mo Yang, A microfluidic flow-through chip integrated with reduced graphene oxide transistor for influenza virus gene detection, Sensors and Actuators B: Chemicalhttp://dx.doi.org/10.1016/j.snb.2017.05.147

A microfluidic flow-through chip integrated with reduced graphene oxide transistor for influenza virus gene detection

Chunyu Chan,[a] Jinyu Shi,[a] Yadi, Fan,[a] and Mo Yang*[a,b]

[a] Interdisciplinary Division of Biomedical Engineering, the Hong Kong Polytechnic University, Hung Hom, Kowloon, Hong Kong, P.R. China

[b] PolyU Shenzhen Research Institute, Shenzhen, P.R. China

*Corresponding author: Dr. Mo Yang, Interdisciplinary Division of Biomedical Engineering, the Hong Kong Polytechnic University, Hung Hom, Kowloon, Hong Kong, P.R. China.

E-mail: Mo.Yang@polyu.edu.hk; Phone: 852-2766-4946; Fax: 852-2334-2429

Highlights

- A novel flow-through microfluidic integrated rGO transistor is developed for H5N1 influenza virus gene detection
- Extended long probe immobilization strategy is demonstrated to have both high stability and sensitivity in the flowing environment
- The limit of detection of 5 pM was achieved with the flow-through approach
- A promising platform for developing graphene transistor based flow-through chips for nucleic acid detection

Abstract

Most of the current graphene transistor based deoxyribonucleic acid (DNA) sensors are based on dip-and-dry methods. The flow-through approach for graphene transistor based DNA sensors have not been explored yet. Moreover, the effect of probe immobilization strategies on the performance of a graphene transistor biosensor in flowing environment was rarely studied. In this paper, a microfluidic integrated reduced graphene oxide (rGO) transistor was developed for H5N1 influenza virus gene detection with high stability and sensitivity via a flow-through strategy. Different DNA

probe immobilization approaches including extended long capture probe via π-π stacking, short capture probe via π-π stacking and covalent immobilization via linker were studied. Both fluorescence measurement and electrical detection were performed to evaluate the performance of rGO transistors in flowing environment for these probe immobilization strategies. The results showed that among these approaches, extended long capture probe could provide both high sensitivity and stability in flowing environment while short capture probe suffered by the low stability in flowing environment and covalent immobilization via linker had relatively low sensitivity. This microfluidic integrated rGO transistor with extended capture probe immobilization approach could provide a promising platform for nucleic acid detection with high sensitivity and stability for potential flow-through chip application.

Keywords: Microfluidic device; Flow-through chip; Reduced graphene oxide (rGO); Transistor

1. Introduction

Biological field-effect transistor (bio-FET) is a promising platform for label-free and rapid detection of biological targets, whose mechanism is based on direct measurement of conductance change induced by the electric potential generated from biological targets binding on the gate surface [1,2]. However, conventional silicon based bio-FET devices have relatively low sensitivities [3,4], which hampers its biomedical applications.

Graphene, a novel two-dimensional single atomic planar sheet, has attracted tremendous interests for various biosensing applications due to its high carrier mobility, large contact area and highly tunable chemical and physical performance [5,6]. Moreover, since graphene atoms in the atomic thin layer are exposed to outside environment, the electrical properties of graphene layer are very sensitive to the binding events of chemical or biological molecules on surface, which makes graphene a potential candidate of bio-FET device for various biological species detection including cell [7], protein [8,9], bacteria [10] and toxin [11]. Many efforts have also been spent on nucleic acid detection using graphene or reduced graphene oxide (rGO) based transistors [12-16]. However, most of the current graphene transistor based nucleic acid biosensors are based on dip-and-dry method, which is simple but easy to be contaminated and not suitable for automation operation. The flow-through approach with graphene transistors for nucleic acid detection is seldom explored, which could provide an enclosed environment to ensure cleanness and also has the potential for automation operation.

One of the key issues for graphene FET based nucleic acid biosensor with flow-through approach is how to realize stable immobilization of nucleic acid probes on graphene surface and preserve the conductivity of graphene for high sensitive detection simultaneously in flowing environment. Traditional covalent functionalization methods such as silane-based modification will cause disruption of graphene aromatic structure and decrease mobility largely, which is generally not adopted for graphene transistor

based biosensors [17]. The current immobilization strategies for graphene transistors with dip-and-dry methods are mainly based on two approaches: direct probe immobilization by π-π stacking and immobilization via linkers with aromatic rings such as pyrenebutyric acid. The direct probe immobilization approach is based on π-π stacking between nucleic acid and graphene surface [12-13, 15]. The approach with probe immobilization via pyrenebutyric acid linker uses the pyrene-end in the linker molecule to strongly bind with the basal plane of graphene via π-π stacking interaction and the other end with carboxyl group to covalently bind with amine group of probes [18,19]. Both approaches can keep the high conductivity of graphene surface without breaking internal crystal structures.

However, for the previous studies using direct probe immobilization approach, capture probes and target have exactly the same length and matching sequence. When complimentary targets hybridize with capture probes, fully matched dsDNA have poor affinity to graphene surface due to the shielding of nucleobases within the negatively charged double-stranded DNA (dsDNA) phosphate backbone [20-22]. The hybridized probes DNA tends to detach from graphene surface by negative charge repulsion between the phosphate group of dsDNA and GO surface which makes this scheme not suitable for DNA detection applications for flow-through chip. Probe immobilization approach via pyrenebutyric acid linkers could ensure the probe stability in the flowing environment. But the linker molecules may increase the distance between target DNA and graphene surface, which may decrease the sensitivity of graphene transistors.

In this paper, a microfluidic integrated rGO transistor with extended long capture probe was developed for potential flow-through chip application. This extended long capture probe was composed of two sections: one section with sequence complementary to target DNA and the extended region was designed for maintaining the π-π stacking interaction between dsDNA and graphene, allowing the probe-target dsDNA complex being retained on rGO surface in the flowing environment. This probe immobilization strategy with extended long capture probe could ensure both high stability and sensitivity in flowing environment. As a demonstration, this rGO microfluidic chip was used for H5N1 avian influenza virus gene sequence detection. The rGO transistor with extended long capture probe was found to provide the best performance with both high stability and sensitivity among those. This microfluidic integrated graphene transistor chip has the potential for developing graphene transistor based flow-through chip for nucleic acid detection in the area of clinical diagnostics, food safety and environmental monitoring.

2. Materials and Methods

2.1 Materials

GO (SKU-GO-W-175, Flake size: 300-700 nm, 5 mg/ml) was purchased from Graphene Supermarket. 1-pyrenebutyric Acid, 3-aminopropyltriethoxysilane (APTES) and hydrazine monohydrate were purchased from Sigma-Aldrich. Silicon wafer (300 nm SiO2 layer on Si) was purchased from MTI Corporation. PDMS (Sylgard 184 silicone elastomer kit) was purchased from Dow Corning. Oligonucleotides were synthesized by Integrated DNA Technologies (IDT)

Inc. (Coralville, IA, US). Oligonucleotide sequences derived from an H5N1 avian influenza are 5'-CCA AGC AAC AGA CTC AAA-3' [24, 25]. The other oligonucleotides used in this experiment include:

Short capture probe (SP): 5'-TTT GAG TCT GTT GCT TGG-3'

Fluorescent-labeled short capture probe: 5'-TTT GAG TCT GTT GCT TGG- Cy3-3'

Extended long capture probe (LP): 5'-GTG TGT GTG TGT GTG TGT GTG TGT GTG TGT TTT GAG TCT GTT GCT TGG-3'

Fluorescent-labeled extended long capture probe: 5'-GTG TGT GTG TGT GTG TGT GTG TGT GTG TGT TTT GAG TCT GTT GCT TGG-Cy3-3'

Amine modified capture probe (NH_2-P): 5'-NH_2 -TTT GAG TCT GTT GCT TGG-3'

Non-Complementary DNA (non-cDNA): 5'-TTA TTC CCT GAA AAA TTG-3'

2.2 Preparation of microfluidic channel integrated rGO transistor

Fabrication procedures of rGO film on a Si/SiO_2 wafer followed the previous report [22]. Briefly, a Si/SiO_2 wafer was firstly activated by piranha treatment and salinized by APTES. Then, GO (5 mg/mL) was allowed to spin at 1600 rpm to generate an uniform and thin film on the substrate followed by dring. Finally, hydrazine reduction was performed overnight at 85^0C. The obtained rGO film was shielded by a hard mask and patterned to a 1 mm width band by plasma treatment. Subsequently, Ti/Au contact pads were sputtered and patterned as contact electrodes. The patterned

rGO channel has the dimension of 4 mm x 1 mm x 0.2 mm. Soft lithography method was then used to fabricate the microfluidic chip. Negative photoresist SU-8 (MicroChem Corp., Newton, MA) was used to fabricate the master on Si wafer. The SU-8 master on Si wafer was then used to generate the PDMS microfluidic channels by thermal curing on a hot plate at 90^0C for 1 hour. To integrate the PDMS layer with graphene transistor on Si/SiO_2 wafer, PDMS layer was first treated with oxygen plasma and then bonded with the Si/SiO_2 wafer with rGO transistor.

2.3 Immobilization and hybridization of DNA on rGO

For π-π stacking based immobilization, the fabricated rGO transistor was firstly functionalized by immobilizing capture probe via π-π stacking interaction between probe and rGO surface. A 20 µL phosphate-buffered saline (PBS) (1X PBS, pH=7.4) solution of 10 µM capture probe (either short probe or long probe) was incubated on the rGO channel overnight at room temperature. Afterwards, the loosely bonded DNA was removed by rinsing with 0.2% sodium dodecyl sulfate (SDS) in PBS solution, PBS solution and deionized (DI) water sequentially.

For pyrenebutyric acid linker based immobilization, a 20 µL 1-pyrenebutyric acid solution (10 mM) in dimethylformamide (DMF) was dropped on the rGO channel and incubated overnight. Afterwards, the rGO channel was rinsed with DMF and DI water in sequence. After air drying, EDC/NHS in 1X 2-(N-morpholino)ethanesulfonic acid (MES) buffer was then applied to activate the rGO channel for 30 mins. Afterwards, a 20 µL amine modified

capture probe (10 μM) was added for covalently bonding to pyrenebutyric acid. After resting overnight, the channel was rinsed by PBS and DI water to remove loosely attached probes.

2.4 Electrical signal measurement and characterization

This rGO transistor based biosensor was measured with a semiconductor parameter analyzer (Keithley 4200). During the measurement, a blank 1X PBS was used as the reference measurement electrolyte. Original conductance (G_0) was defined as the channel conductance when 1X PBS was added into the sample chamber. Device response was calculated as the relative conductance change $\Delta G/G_0$.

2.5 Characterization

AFM experiment of rGO morphology was performed with a multifunctional Scanning Probe Microscopy (Digital Instruments NanoScope IV). Raman spectra of GO and rGO were measured by a Horiba Jobin-Yvon Raman system (LabRam HR800) equipped with a 488 nm laser excitation source. X-ray photoelectron spectroscopy (XPS) experiment was performed with a Leybold Heraeus SKL-12 spectrometer modified with VG CLAM 4 multichannel hemispherical analyzer. Fluorescent experiments were performed with a Tecan Infinite F200 microplate reader.

3. Results

3.1 Mechanism of extended long capture probe immobilization in flow environment

Fig. 1 shows the mechanism of extended long capture probe immobilization strategy

to keep probe stability in the flow environment. The extended long capture probe was composed of two sections: one section with sequence complementary to target DNA and the extended region was designed for maintaining the π-π stacking interaction between DNA and graphene, allowing the probe-target dsDNA complex being retained on rGO surface. As shown in Fig. 1a, both sections of extended long capture probes originally adhere to rGO surface via π-π stacking. When complimentary targets hybridize with capture section of the long probes, the hybridized dsDNA part loses the adhesion force while the immobilization section still keeps the adhesion force via π-π stacking. A PDMS microfluidic chip integrated with rGO transistor was designed for testing the stability of probes with various immobilization strategies (Fig. 1b). As shown in Fig. 1c, in the flowing environment, short capture probes with fully matching sequence will detach and be washed away from rGO surface after hybridization with complimentary targets due to the shielding of nucleobases within the negatively charged dsDNA phosphate backbone. In contrast, extended long capture probes will remain on rGO surface due to the adhesion force from immobilization section with rGO surface in the flowing environment, which can ensure the stability in the flow-through approach in microfluidic devices.

3.2 Preparation and characterization of rGO films on Si/SiO_2 substrate

A large area and continuous GO film with few layers was obtained on a Si/SiO_2 substrate by the spin-coating method. The rGO film was then obtained by using hydrazine vapor reduction. As shown in the AFM image (Fig. 2a), the size of most rGO sheets are in the range of 500 nm to 1 μm. This continuous rGO film is composed of single layer of rGO sheets

and two to three overlapping layers of rGO sheets with the thickness from 1-4 nm. The reduction process from GO to rGO was characterized by Raman spectroscopy (Fig. 2b). Well defined D and G bands can be observed from Raman spectra with D band at ~ 1350 cm^{-1} and G band at 1580 cm^{-1}. The relative ratio of D and G band intensity (I_D /I_G) of GO increased from 0.89 (GO) to 1.20 (rGO) which demonstrated the successful reduction process.

Detailed chemical components of GO and rGO were further investigated by X-ray photoelectron spectroscopy (XPS). As shown in Fig. 2c, the oxygen content of GO represented by O_{1s} peak at 534 eV decreased significantly after reduction and carbon content represented by C_{1s} at 286 eV increased obviously after reduction. Fig. 2d and Fig. 2e shows XPS C_{1s} scans which consisted of different components including C-C, C-O, C=O and C(O)O. After reduction, the C-C bond became much stronger than the other oxygen related bonds in GO sheets which also demonstrated the successful reduction of GO.

3.3 Comparison of the affinity to rGO surface for long capture probe and short capture probe

To compare the hybridized probes stability under flowing environment in the microfluidic channel, two types of capture probes including extended long capture probe (LP) and short capture probe (SP) with the same concentrations were used for testing the affinity to rGO surface. LP has one section of base-pair sequence complementary to target and the other extended section with the function of adhering to rGO surface even after hybridization. In contrast, SP only has fully matching sequence with target. Both LP and SP were modified with Cy3 fluorescence tags at 3' end. LP and SP solutions with the same concentration (10 μM)

were first incubated with rGO surfaces and then washed with PBS solution. A volume of 1 mL solution with 10 μM complimentary DNA (cDNA) or non-cDNA was then injected into the chamber by the syringe pump. After incubation, the solutions were removed and PBS solution was injected to wash the rGO surfaces by the syringe pump with a flowing velocity of 40 uL/min for one minute. The fluorescence signals of removed solutions were then measured off-chip using a microplate reader.

Fig. 3 shows the normalized fluorescence signals for four cases of SP + cDNA, SP + non-cDNA, LP + non-cDNA and LP + cDNA. Here, the fluorescence signal of SP + cDNA was used as the reference. It was observed that the SP + cDNA case had the highest fluorescence signal. Fully complementary dsDNA was formed after hybridization and it was released from rGO surface generating fluorescence signal in the solution. The fluorescence signal observed in this experiment suggested that the fully hybridized SP-cDNA complex was not stably adhered on rGO and gentle washing liberated the dsDNA into the solution phase. SP + non-cDNA and LP + non-cDNA had a relatively low fluorescence signal in the solution because SP/ LP did not hybridize with non-cDNA and most fluorescence-labeled SP/LP stayed on rGO surface. Hence fluorescence signal could barely be found in the solution. Non-specific displacement of fluorescence-labeled LP and SP on rGO surface was not obvious. A little higher fluorescence signal was also found in the case of LP + cDNA compared with LP + non-cDNA and SP + non-cDNA due to the partial dissociation of target sequence. For LP + cDNA case, cDNA only hybridized with half of LP and the extended part of LP was still immobilized on rGO surface via π-π interaction. The partially hybridized LP-cDNA double-stranded complex was confined on

the surface of rGO due to the π-π interaction of the extended LP end. The extended end of LP provided a better affinity with rGO and the immobilization remained even after target hybridization.

This experiment demonstrated that extended long capture probe is more stable on rGO surface after hybridization with cDNA in the flowing environment. Such stable immobilization scheme is crucial for developing a flow-through chip with graphene transistor for DNA detection. In contrast, detachment of SP-cDNA decreased the cDNA capturing rate and sensitivity, making it an undesirable immobilization strategy for a microfluidic integrated graphene transistor chip.

Here Fig. 3

3.4 rGO FET with extended long capture probe for target detection

To investigate the functionality of this microfluidic integrated rGO transistor chip with LP, drain-source I-V curves were recorded for H5N1 influenza virus gene detection. 100 µL of the cDNA sample was injected into the microfluidic chip through the inlet port with a flow rate of 2 µL/min by a syringe pump. Next, 50 µL 1X PBS solution containing 0.2% sodium dodecyl sulfate (SDS) was injected into the microfluidic chip with a flow rate of 5 µL/min to remove the weakly bound cDNA. Finally, 1X PBS was injected into the measuring chamber as the reference measurement electrolyte. Fig. 4a shows the I-V curves of bare rGO, rGO functionalized with LP and rGO functionalized with LP after cDNA hybridization. When the gate of rGO FET was immobilized with LP, the conductance decreased which indicated the

successful immobilization of LP on rGO surface. With the hybridization with cDNA, the conduction further decreased. This trend agreed with previous studies in the literature that DNA adsorption on rGO thin film led to n-doping effect to decrease rGO conductance [23]. The capture of cDNA brought more negatively charged DNA phosphate backbone to the proximity of rGO which further decreased the channel conductance. In contrast, the addition of non-cDNA brought a less observable conductance decrease due to the lack of hybridization between LP and non-cDNA (Fig. 4b). Slight decrease of rGO conductance was due to non-specific absorption of a small amount of non-cDNA on rGO surface.

Here Fig. 4

3.5 Electrical detection with various probe immobilization approaches

We also compared the sensitivity of this transistor biosensor in microfluidic channel flowing environment with three probe immobilization strategies: SP, LP and covalent immobilization of amine modified capture probes (NH_2-P) via bifunctional linker (pyrenebutyric acid). To achieve covalent attachment of NH_2-P on rGO surface, pyrenebutyric acid was firstly linked with rGO surface via π-π stacking interaction. NH_2-P was then covalently immobilized on rGO using EDC/NHS method. Fig. 5 shows the relative conductance change of rGO transistors with SP, LP and pyrenebutyric acid linker at various cDNA concentrations (from 10 pM to 1 μM) in the same microfluidic flowing environment. Compared with absolute conductance change (ΔG), the relative conductance change ($\Delta G/G_0$) is a better indicator for the sensitivity of the device which could eliminate the effect of variation in initial conductance

G_0. Obviously, rGO transistors modified with LP have much larger conductance change and higher sensitivity in the microfluidic flowing environment compared with those with SP and pyrenebutyric acid linker. This can be explained by the following reasons. Generally, the sensitivity of rGO transistor in flowing environment is determined by two parameters: the distance between the probes and graphene surface and the stability of probes. Firstly, when target oligos hybridized with LP/SP, they were brought to the proximity of rGO surface leading to decrease of conductance by the n-doping effect. In contrast, the distance between hybridized target oligos and rGO surface via pyrenebutyric acid liner was much larger than LP method which led to the small effect on conductance change. Secondly, LP approach has better stability for retaining probe-cDNA complex on the surface compared with SP approach. When cDNA binds with SP on rGO surface, some SP-cDNA complexes detach from the surface and the generated vacancies on the surface may be replaced by the free cDNA in the solution. The mixed effects of SP-cDNA binding on rGO surface, the detachment SP-cDNA complex and the vacancy replacement with free c-DNA in solution lead to the small conductance change of rGO surface. In contrast, LP-cDNAs complexes stays on the rGO surface during the binding process between cDNAs and long probes. This continuous LP-cDNAs formation on rGO surface leads to a large conductance decrease of rGO surface due to the N-doping effect of DNA. The limit of detection (LOD) with LP approach in the flowing-through chip is around 5 pM, which is determined by the control signal plus three times of noise signal (standard derivation). This LOD of 5 pM in flowing-through chip is comparable to those of reported graphene transistor based DNA sensors with dip-and dry approaches, which are in the range from 100 fM to 10

pM [13, 15, 23]. The results demonstrated that the graphene transistor with extended long probe approach really could provide high sensitivity and stability in flow-through chip.

Here Fig. 5

3.6 Specificity testing with LP approach

The above experiments demonstrated LP was the best choice among those three probe immobilization approaches. The specificity of this microfluidic integrated rGO transistor chip modified with LP was also tested with cDNA and non-cDNA. I_{ds} was recorded to analyze the conductance change ($\Delta G/G_o$) of rGO transistor during hybridization process. Fig. 6 shows the relative conductance change of rGO transistor with LP at various cDNA or non-cDNA concentrations in the microfluidic chip. Generally, there is an obvious difference between the conductance change between cDNA and non-cDNA for all the target concentrations which demonstrated the specificity of this microfluidic integrated rGO transistor sensor. A linear relationship between relative conductance change and the logarithm of cDNA concentrations was found in the range from 10 pM to 100 nM with the corresponding equation $y = -0.258\ln(x) -0.6021$ and $R^2 = 0.9731$.

Here Fig. 6

4. Conclusion

In this paper, a microfluidic integrated rGO transistor chip was developed for H5N1 influenza virus gene detection in flowing environment. Different DNA probe immobilization approaches including extended long capture probe via π-π stacking,

short capture probe via π-π stacking and covalent immobilization via linker, were explored for the probe stability after hybridization and the related effects on sensitivity of rGO transistors in flowing envionment. The results showd that rGO transistor with extended long capture probe approach had the best performance with high stability and sensitivity in the flow-through chip. In contrast, short probes with fully complementary sequence with cDNA had a relatively high chance of detachment after hybridization since the dsDNA structure shielded the base pairs and weakened π-π interaction force. Covalent immobilization by bifunctional linker pyrenebutyric acid was reliable, but had relatively low sensitivity due to the long distance by the linker spacer between captured target and graphene surface. The high stability and sensitivity of extended long capture probe approach could be attributed to the extended immobilization section with high affinitiy to rGO surface after hybridization and the close distance between LP-cDNA and rGO since no spacer was involved.

The current dominating method for influenza virus detection is reverse-transcriptase polymerase chain reaction (RT-PCR), which is quite sensitive with the limit of detection (LOD) in the femtomolar level but requires expensive apparatus and well-trained technicians to perform the test in a laboratory environment with 4-8 hours [27]. Various sensing approaches for influenza virus gene detection have been developed including electrochemical sensing [28] and fluorescence based nuclide acid assay [29], which have LOD in the pM level and the detection time around 2- 4 hours. Our rGO transistor sensor achieved a LOD of 5 pM with the detection time around 1 hour via flow-through approach,

which is comparable to the current biosensing appraoches with shortened detection time. This microfluidic integrated rGO transistor with extended long capture probe immobolization approach could provide a promising platform for nucleic acid detection for potential flow-through chip application with high sensitivity and stability.

Acknowledgement

This work was supported by the National Natural Science Foundation of China (Grant No.:81471747), the Hong Kong Research Council General Research Grant (PolyU 152213/15E) and the Central Research Grant of the Hong Kong Polytechnic University (Grant No: G-YBAA) and Internal Fund of the Hong Kong Polytechnic University (Grant No: 4-BCCC).

References

[1] U.Brand, B. Reinhardt, F. Ruther, T. Scheper, K. Schugerl, Sens. Actuator B-Chem., 4(1991), 315-318.

[2] R.X. He, M. Zhang, F. Tan, P. H. M. Leung, X.Z. Zhao, M. Yang and F. Yan, Journal of Materials Chemistry, 22(2012), 22072-22076.

[3] L. Kergoat, B. Piro, M. Berggren, G. Horowitz, M.C. Pham, Anal. Bioanal. Chem., 402(2012), 1813-1826.

[4] C.S. Lee, S.K. Kim, M. Kom, Sensors, 9(2009), 7111-7131.

[5] A.K. Geim, Science, 324(2009), 1530–1534.

[6] J.Shi, J.Guo, G. Bai, C. Chan, X. Liu, W. Ye, J. Hao J, S. Chen, M. Yang. Biosens Bioelectron. 65(2015), 238-44.

[7] T. Cohen-Karni, Q. Qing, Q. Li, Y. Fang, C.M. Lieber, Nano Lett. 10(2010), 1098–1102.

[8] T. Kuila, S. Bose, P. Khanra, A.K. Mishra, N.H. Kim, J.H. Lee, Biosens. Bioelectron., 26(2011), 4637-4648.

[9] Y. Ohno, K. Maehashi, K. Matsumoto, J. Am. Chem. Soc., 132(2010), 18012–18013.

[10] Y.X. Huang, X.C. Dong, Y.X. Liu, L.J. Li, C. Peng, J. Mater. Chem., 21(2011), 12358-12362.

[11] D.J. Kim, H.C. Park, I.Y. Sohn, J.H. Jung, O.J. Yoon, J.S. Park, M.Y. Yoon, N.E. Lee, Small, 9(2013), 3352-3360.

[12] R. Stine, J.T. Robinson, P.E. Sheehan, C.R. Tamanaha, Adv. Mater., 22(2010), 5297-5300.

[13] Z.Y. Yin, Q.Y. He, X. Huang, J. Zhang, S.X. Wu, P. Chen, G. Lu, P. Chen, Q.C. Zhang, Nanoscale, 4(2012), 293-297.

[14] T.T. Chen, P.T. Loan, C.L. Hsu, Y.H. Lee, J. Tse-Wei Wang, K.H. Wei, C.T. Lin, L.J. Li, Biosens Bioelectron., 15(2013), 103-109.

[15] X.H. Zhang, Y. Zhang, Q.L.Y. Liao, S.W. Ma, Small, 9(2013), 4045-4050.

[16] C.T. Lin, P.T.K. Loan, T.T. Chen, K.K. Liu, C.H. Chen, K.H. Wei, L.J. Li, Advanced Functional Materials, 23(2013), 2301-2307.

[17] V. Georgakilas, M. Otyepka, A.B. Bourlinos, V. Chandra, N. Kim, K.C. Kemp, P. Hobza, R. Zboril, K.S. Kim, Chem. Rev., 11(2012), 6156-6214.

[18] S.R. Guo, J. Lin, M. Penchev, E. Yengel, M. Ghazinejad, C.S. Ozkan, M. Ozkan, J Nanosci Nanotechnol., 11(2011), 5258-5263.

[19] E. Pembroke, G.D. Ruan, A. Sinitskii, D.A. Corley, Z. Yan, Z.Z. Sun, J.M. Tour, Nano Res. 6(2013), 138-148.

[20] C.H. Lu, H.H. Yang, C.L. Zhu, X. Chen, G.N. Chen, Angew. Chem. Int. Ed. 48(2009), 4785-4787.

[21] Y.X. Liu, F. Liu, T.S. Seo, Chem. Commun., 47(2011), 12149-12151.

[22] P.J.J. Huang, J.W. Liu, Small, 8(2012), 977-983.

[23] J.F. Ou, J.Q. Wang, S. Liu, B. Mu, J.F. Ren, H.G. Wang, S.R. Yang, Langmuir, 26(2010), 15830–15836.

[24] X.C. Dong, Y.M. Shi, W. Huang, P. Chen, L.J. Li, Adv. Mater., 22(2010), 1649-1653.

[25] J. Pipper, M. Inoue, L. F-P-Ng, P. Neuzil, Y. Zhang, L. Novak, Nature Medicine 13(2007), 1259–1263

[26] B.P. Ting, J. Zhang, Z. Gao, J.Y. Ying. Biosens Bioelectron. 25(2009), 282-287.

[27] B. Hoffmann, T. Harder, E. Starick, K. Depner, O. Werner, M. Beer, J. Clin. Microbiol. 45(2007), 600-603.

[28] K. Malecka, A. Stachyra, A. Gora-Sochacka, A. Sirko, W。 Zagorski-Ostoja, H. Radecka, J. Radecki, Sensors and Actuators B: Chemical, 224(2016), 290-297

[29] W.W. Ye, M.K. Tsang, X. Liu M. Yang, J.H. Hao, Small, 10(2014), 2390-2397.

Biographies

Chun-Yu Chan received B.S. degree from Hong Kong University of Science and Technology in 2009, M.Sc. degree from the Hong Kong Polytechnic University in 2012 and Ph. D degree in 2015. His research interests include nanomaterials based electrochemical biosensors.

Jingyu Shi received the B.S. degree from Sichuan University, China in 2012, Mphil degree from the Hong Kong Polytechnic University in 2015. She is currently a Ph. D student in Interdisciplinary Division of Biomedical Engineering of the Hong Kong Polytechnic University since 2015. Her research interests include nanoparticle based FRET biosensor for DNA and biomolecule detection.

Yadi Fan received the B.S. degree from Jianghan University, China in 2015, MSc degree from the Hong Kong Polytechnic University in 2016. She is currently a research assistant in the Interdisciplinary Division of Biomedical Engineering of the Hong Kong polytechnic University. Her research interests include 2D nanomaterials based nanoprobe for cell imaging.

Mo Yang received the B.Eng. and M.Sc. degrees in Power Mechanical Engineering from Shanghai Jiaotong University, Shanghai, China, in 1998 and 2001, respectively. He received the Ph.D. degree in Mechanical Engineering from the University of California, Riverside, in 2004. Currently, he is an Associate Professor in Interdisciplinary Division of Biomedical Engineering of the Hong Kong Polytechnic University. His research interests include nanomaterial based biosensing and bioimaging, microfluidics and instrumentation of biomedical micro-devices.

Figure Captions

Fig. 1 Mechanism of extended long capture probe immobilization strategy to keep probe stability in the flow environment. (a) The immobilization section of extended long capture probe still keep π-π stacking interaction on rGO surface after hybridization; (b) The PDMS microfluidic integrated rGO transistor chip; (c) In flowing environment, short capture probes with fully match sequence after hybridization with target are washed away from rGO surface. Extended long capture probes are still kept on rGO surface.

Fig. 2 (a) AFM image and height profile of rGO film on Si/SiO_2 substrate; (b) Raman spectroscopy of GO film and rGO film after hydrazine reduction; (c) XPS wide scan spectra of GO and rGO after reduction; XPS wide scans for C_{1s} of (d) GO and (e) rGO.

Fig. 3 Fluorescence signals of removed samples in the washing environment for four cases of (a) SP + cDNA, (b) SP + non-cDNA, (c) LP + cDNA, and (d) LP + non-cDNA. Here, the fluorescence signal of SP + cDNA was used as the reference.

Fig. 4 Direct current measurement for (a) cDNA and (b) non-cDNA for bare rGO, rGO functionalized with LP and rGO functionalized with LP after target addition.

Fig. 5 Relative conductance change ($\Delta G/G_0$) of rGO transistors with different probe immobilization approaches of short probes, extended long capture probes and covalent immobilization with linkers in various cDNA concentrations in the microfluidic chip after washing steps.

Fig. 6 Relative conductance change ($\Delta G/G_0$) of rGO transistors with LP at various cDNA and non-cDNA concentrations in the washing environment. Inset: linear detection range of rGO transistor using LP.

Figr-1

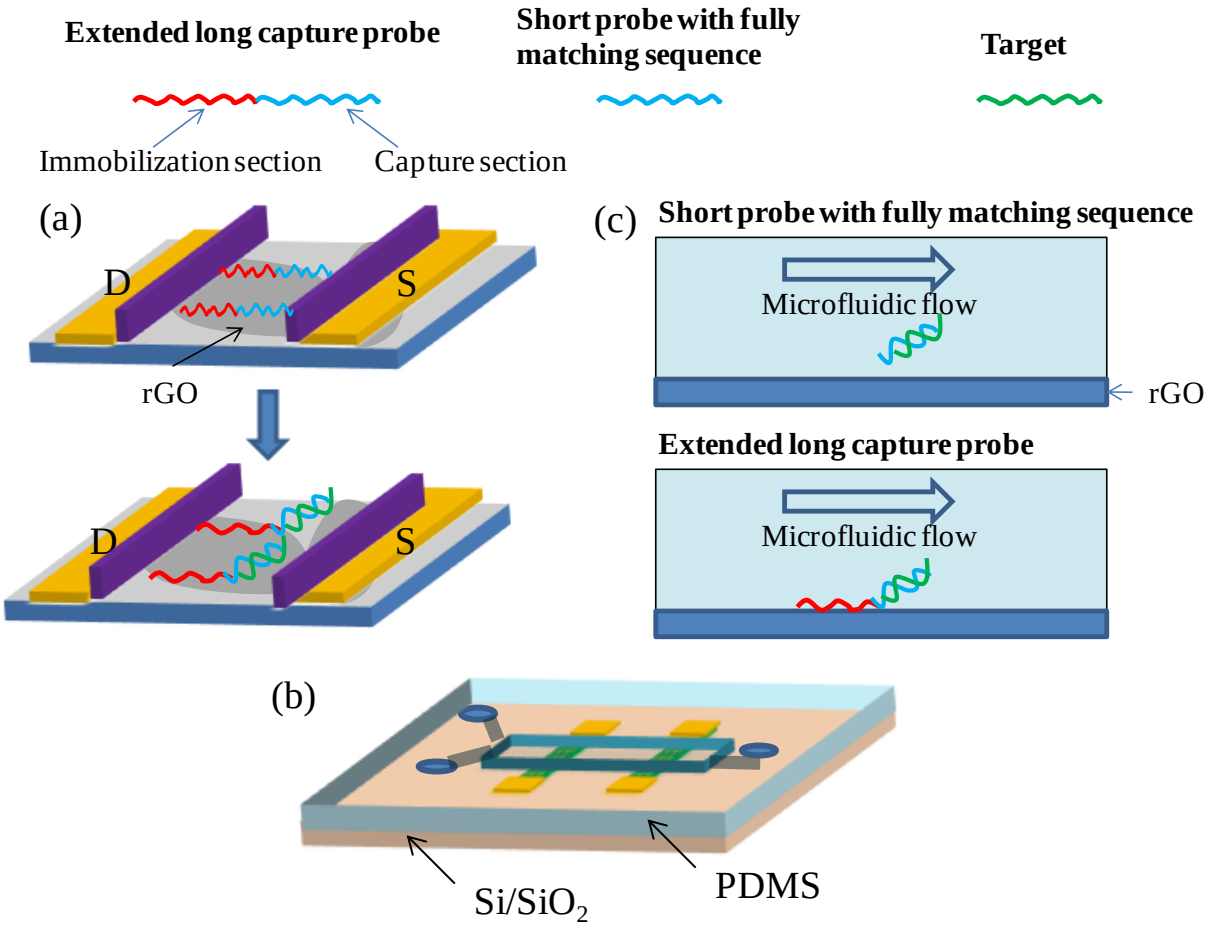

Figr-2

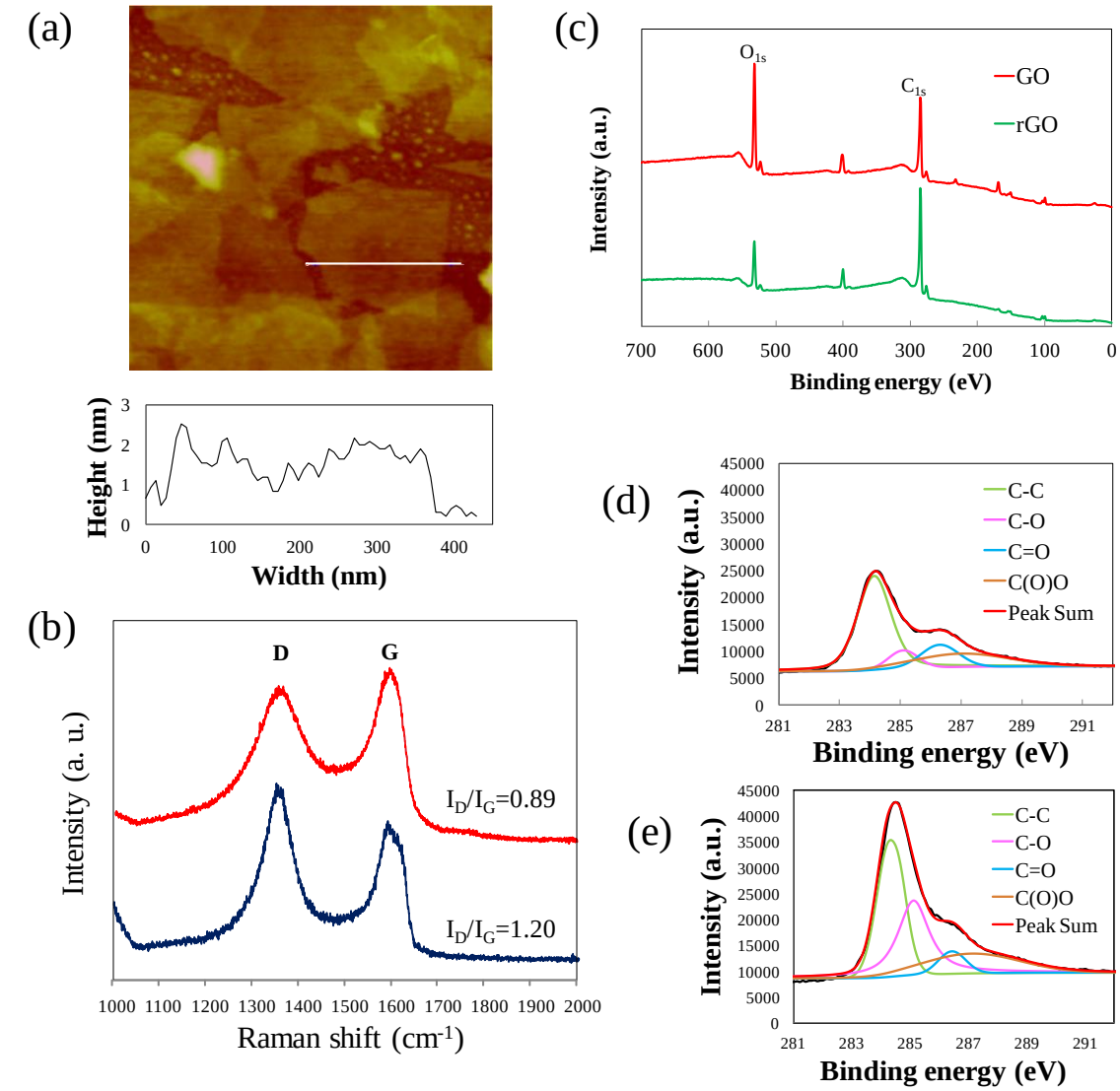

Figr-3

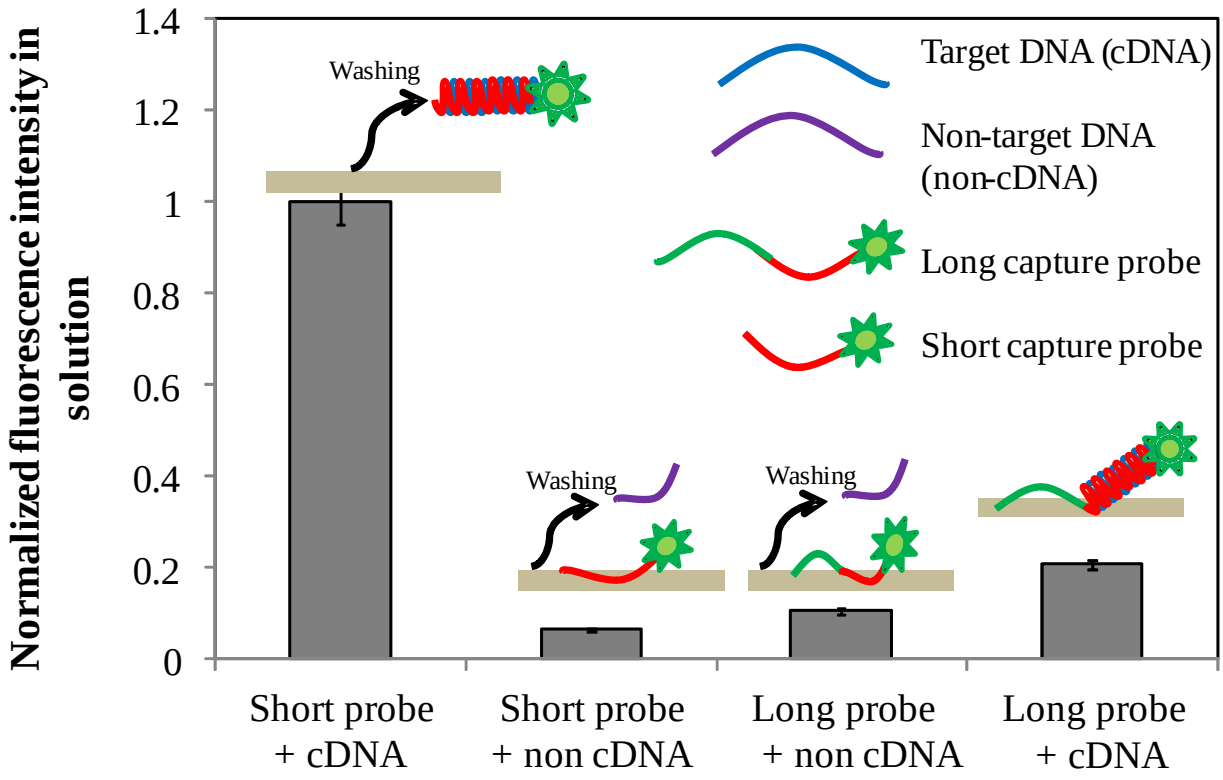

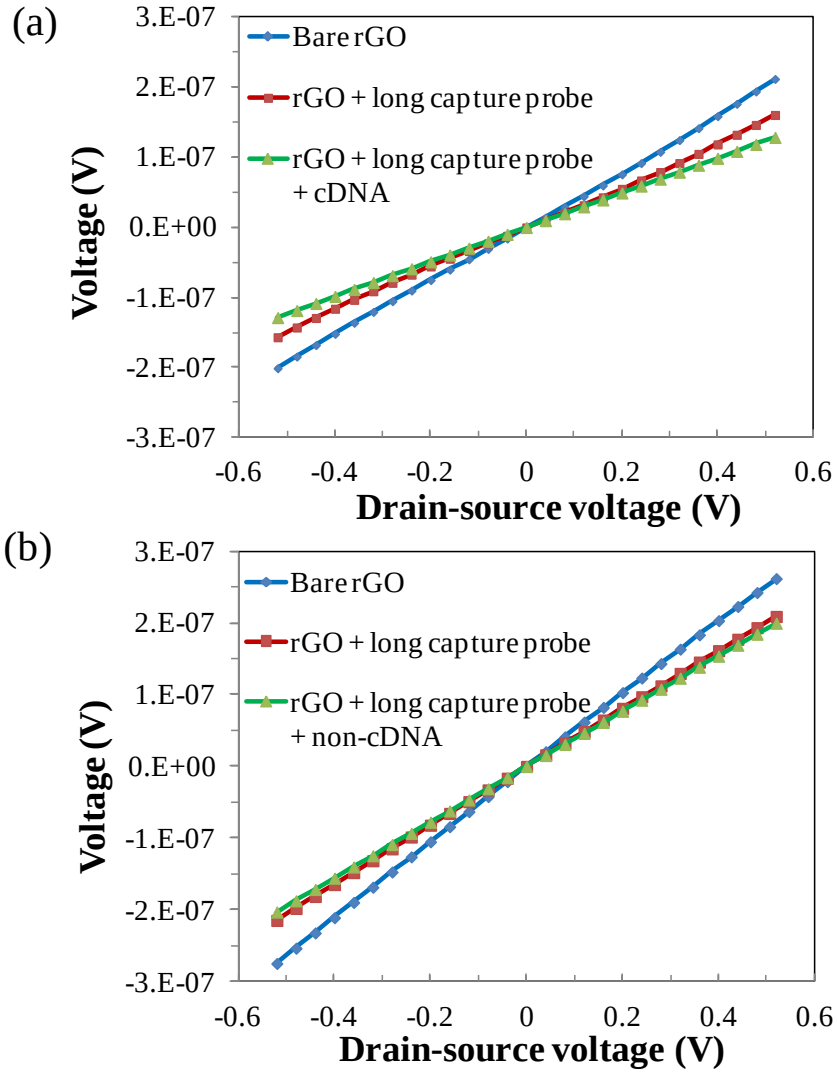

Figr-4

Figr-5

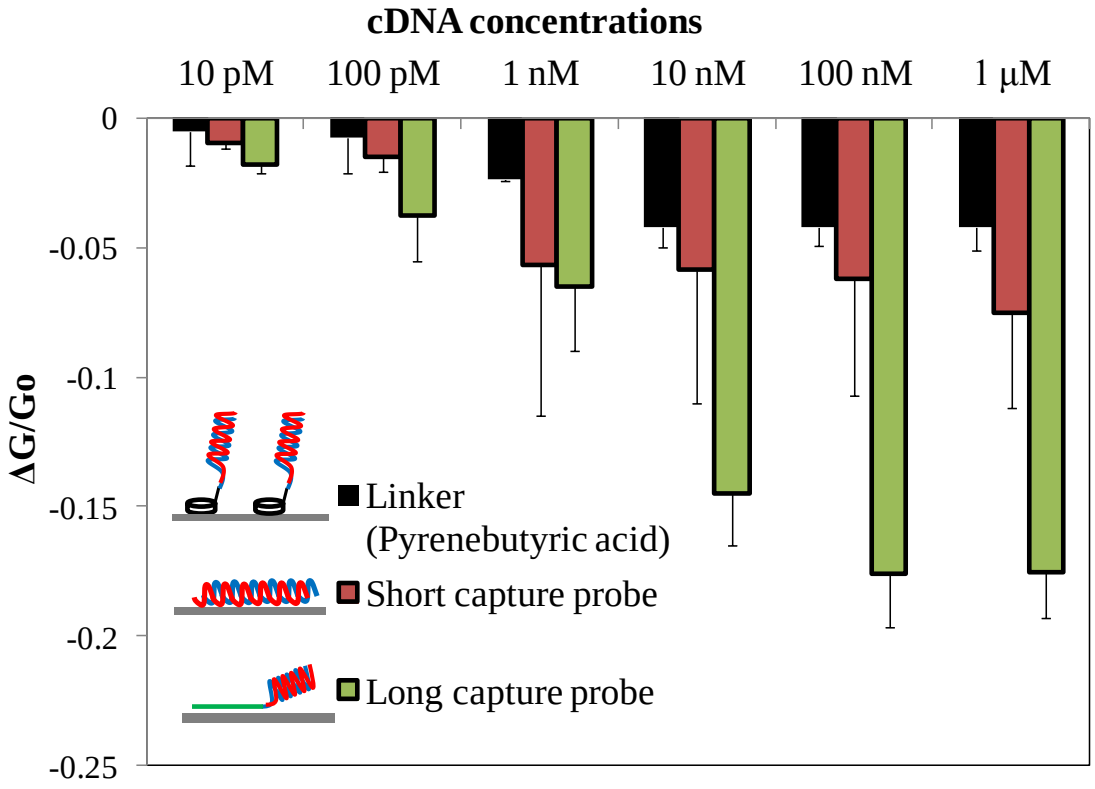

Figr-6